Histol Histopathol (2008) 23: 953-964

http://www.hh.um.es

Histology and Histopathology

Cellular and Molecular Biology

Defect of the cerebellar vermis induced by prenatal γ-ray irradiation in radiosensitive BALB/c mice

Aya Saito[1], Hirofumi Yamauchi[1], Yuka Ishida[2], Yasushi Ohmachi[2] and Hiroyuki Nakayama[1]

[1]Department of Veterinary Pathology, Graduate School of Agricultural and Life Sciences, the University of Tokyo, Japan and [2]Research Center for Radiation Protection, National Institute of Radiological Sciences, Japan

Summary. The developing fetal brain is one of the most susceptible organs to irradiation insult. Prenatal irradiation-induced abnormalities in the cerebrum have been well examined in mouse fetuses. However, little information on abnormalities in the cerebellum caused by irradiation is available. Moreover, few reports have examined the chronological changes of the brain from the prenatal to the postnatal period. To analyze the chronological changes induced by irradiation, we exposed pregnant mice to γ-ray irradiation on embryonic day 13.5 (E13.5) and investigated the histopathology of the cerebellum at several time points from E14.5 to postnatal day 28. BALB/cA mice were used, which is a radiosensitive strain, and C57BL/6J, which is a radioresistant strain. The irradiated BALB/c showed a remarkable vermis deficit after birth, and histological analysis demonstrated that there were severe losses of the external germinal layer (EGL) and Purkinke cell layer. TUNEL analysis shoed that apoptosis was strongly induce in the cerebellar anlage of the irradiated BALB/c compared to the C57BL/6J at E14.5. Immunohisto-chemical analysis revealed a significat decrease of phospho-histone H3 positive EGL cells in the irradiated BALB/c at E18.5 and E0, indicating that irradiation causes a decrease in the number of mitotic cells. The results suggest that the strong induction of apoptosis in radiosensitive BALB/c led to a decrease of proliferation activity in the cerebellar anlage during embryonic development, and consequently, severe cerebellar abnormality was evoked.

Key words: γ-ray, Prenatal irradiation, Cerebellar development, Vermis, BALB/c mice

Offprint requests to: Aya Saito, Department of Veterinary Pathology, Graduate School fo Agricultural and Life Sciences, the University of Tokyo, 1-1-1 Yayoi, Bunkyo-ku, 113-8657 Tokyo, Japan. e-mail: a-saitou@umin.net

Introduction

The developing brain is one of the most susceptible organs to external stimuli, such as ionizing radiation and chemical exposure, because of its long-lasting developing period, which extends from the beginning of embryonic organogenesis to the postnatal infantile period. In particular, the brains of fetuses show the highest sensitivity to prenatal irradiation and suffer from various developmental abnormalities (Kameyama et al. 1972; Kameyama and Hoshino, 1986; Hoshino and Kameyama, 1988). Prenatal exposure to ionizing radiation induces not only early changes soon after the exposure, such as apoptosis of neuronal cells, abnormal cell proliferation/migration, but also late abnormalities, such as macroscopic malformations, reduced brain weight, and neuronal heterotopias (Fukui et al., 1991). A few reports have dealt with the relationship between early lesions and late abnormalities (Sun et al., 1995; Aolad et al., 2000; Kubota et al., 2000). However, as far as we know, there has been no observation of the consecutive changes from the prenatal to postnatal period induced by prenatal irradiation.

Many previous reports on the effect of in utero radiation exposure have focused on cerebral abnormalities, and therefore, details of cerebellar abnormalities induced by irradiation remain unclear. The developmental system of the cerebellum is unique compared to other components of the central nervous system. Neuronal populations of the cerebellum arise from at least two different germinal zones: ventricular zone (VZ) and external germinal layer (EGL). Purkinje cells and neurons in the cerebellar nuclei arise from the former and granule cells, stellate cells and basket cells from the latter. Purkinje cells then migrate from the VZ to the surface of the cerebellar just beneath the

Abbreviations: VZ: ventricular zone, EGL: external germinal layer, PCL: Purkinje cell layer, pH3: phospho-Histone H3, Shh: sonic hedgehog

molecular layer. In contrast, neuronal progenitor cells in EGL migrate from the surface toward the deep cerebellar cortex, finally forming a complex neuronal network (Miale and Sidman, 1961; Altman, 1972, Altman and Bayer, 1978, 1985; Hatten, 1999). This is a unique characteristic of the cerebellum and is quite different from that of the cerebrum. For this reason, a study that focuses on the effect of radiation on cerebellar development is particularly required.

No previous reports have examined the obvious macroscopic abnormalities of the cerebellum induced by early prenatal irradiation. Kameyama et al. concluded that cerebellar abnormalities are induced only by external causes insulted at around birth (Kameyama, 1982). However, it is possible that prenatal irradiation induces macroscopic cerebellar abnormalities, because the cerebellar anlage starts to develop around 9 days after fertilization. Moreover, it is also unclear how strain differences of radiosensitivity of the mouse fetuses influence the cerebellar abnormalities. In the present report, we investigated pathological changes of the cerebellar development caused by irradiation at a highly radiosensitive stage in telencephalic embryogenesis of the mouse (Kameyama, 1982; Hoshino and Kameyama, 1988), and also a stage of formation of the two major cell layers in the cerebellum, i.e., Purkinje cell and granule cell layers (Hatten 1999; Sotelo 2004). We used a radiosensitive strain of BALB/c mice and a radioresistant C57BL/6J.

Materials and methods

Animals

The animals used were C57BL/6J Jcl and BALB/cA Jcl pregnant mice (Japan CLEA, Tokyo, Japan). They were housed in an air-conditioned room (2±1 and a relative humidity of 55±5% with a 12-hour light-dark cycle. The pregnancies were dated from embryonic day 0 (E0) at the first midnight after mating. All procedures were approved by the Animal Care and Use Committee of the Graduate School of Agricultural and Life Sciences, the University of Tokyo, and by the Institutional Committee for Animal Safety and Welfare of the National Institute of Radiological Sciences.

γ-ray irradiation

Sixty six pregnant females per each strain were assigned to two groups: non-irradiated control and 1.5 Gy γ-ray irradiated groups. They were irradiated at E13.5 in their whole body. Exposure to ^{137}Cs-gamma-ray was conducted with Gammacell (Nordion, Ottawa, Canada). Three animals per each group were sacrificed at E14.5, E16.5, E18.5, postnatal day 0 (P0), P3, P7, P10, P14, P21 and P28.

Tissue preparation

Pregnant mice or pups were anesthetized with ether and sacrificed by cervical dislocation at each time point. The brains were removed and fixed in 10% neutral-buffered formalin solution. The tissue samples were embedded in paraffin, sectioned with a microtome at 4 to 6 μm thick. Tissues of the samples of every time point were applied for hematoxylin and eosin (HE) stain, TdT-mediated dUTP-biotin nick end labeling (TUNEL) stain, and phospho-Histone H3 immunostain.

TUNEL stain

In order to observe apoptotic cells twenty-four hours after irradiation, we used a commercial TUNEL kit (Apop Tag Peroxydase In Situ Apoptosis Detection kit, CHEMICON International, Temecula, CA) in accordance with manufacturer's instructions. One section each for three fetuses per dam were randomly chosen, and the number of TUNEL positive cells and total cells were counted under a light microscope (400), within an area of 3.0×10^4 μm^2 in VZ. Percentages for TUNEL positive cells per total cells were presented as the mean ± standard deviation (SD) of three dams. Student's *t*-test was performed for the irradiated BALB/c vs. the irradiated C57BL/6J, and a *p*-value of <0.05 was considered significantly different.

Immunohistochemistry

Phospho-histone H3 (pH3) is expressed during mitosis in a cell cycle, and was used as a proliferating cell marker in the present study. Immunostaining was conducted using an anti-pH3 antibody (1:150, Cell Signaling Technology, Danvers, MA) with LSAB method. In brief, paraffin sections were deparaffinized and autoclaved for 10 min at 121°C in 10mM citrate buffer, pH 6.0. The sections were placed in 0.3% H_2O_2 for 30 min, the sections were reacted with primary antibody at 4°C overnight, with secondary antibody at room temperature for 40 min, and then with peroxidase-labeled streptoavidine DakoCytomation, Glostrup, Denmark) at room temperature for 40 min. The sections were visualized by peroxidase-diaminobenzidine (DAB) reaction and then counterstained with methyl green (DakoCytomation). One section each for two fetuses per dam were randomly chosen and the number of pH3 positive cells and total cells were counted as previously mentioned in TUNEL stain. The percentages for positive cells per total cells were presented as the mean ± SD of two dams. Student's *t*-test was performed for the irradiated groups vs. control groups in the same strain at each time point, and a *p*-value of <0.05 was considered significantly different.

Measurement of the thickness of hemispheres and vermis

The thickness of cerebellar vermis and hemispheres at E14.5 to P0 were measured in HE stained cross sections showing approximately lobule III. Two or three fetuses per dam were used. As shown in Fig. 3a, the

thickness was expressed as the length from the ventral base to the dorsal surface of the cerebellum. The thickness was measured under a light microscope (x 400) with a micrometer inset into the eyepiece. Results were presented as the mean ±SD of two dams per each time point. Student's *t*-test was perfomed for the irradiated groups vs. control groups in the same strain at each time point, and a *p*-value of <0.05 was considered significantly different.

Results

Gross appearance

At P3, no changes were noted in either control or irradiated C57BL/6J (Fig. 1a,c), or in control BALB/c mice (Fig. 1b). On the other hand, a midline part of the cerebellum of the irradiated BALB/c showed remarkable hypoplasia, and the vermis could not be observed (Fig. 1d).

At P28, the vermis formation was almost completed in control BALB/c mice (Fig. 2b), and also in both control and irradiated C57BL/6J (Fig. 2a,c). On the other hand, the irradiated BALB/c had a severe vermis defect (Fig. 2d). Cerebellar hemispheres of both sides protruded into the midline part and touched each other, as if to compensate for the deficit of the vermis. Moreover, at the location where the posterior part of the cerebellum contacted with an anterior part of a medulla oblongata, there was an aperture that reached the fourth ventricle (data not shown). There was no difference in the length along the longitudinal axis of the cerebellum, despite the wide-ranging vermis defect in irradiated BALB/c mice.

In the cerebrum of the irradiated BALB/c, the thickness of the cortex reduced remarkably and the lateral ventricles were dilated, showing an appearance of severe hydrocephalus (Fig. 2d, arrows). The same changes were observed in the irradiated C57BL/6J, but the lesions were milder than BALB/c.

Histology

At E14.5, there were no morphological differences between the cerebella of the two strains or of non-irradiated and irradiated mice. However, a number of pyknotic cells were observed in the ventricular zone (VZ) of irradiated BALB/c (Fig. 5d), and these cells

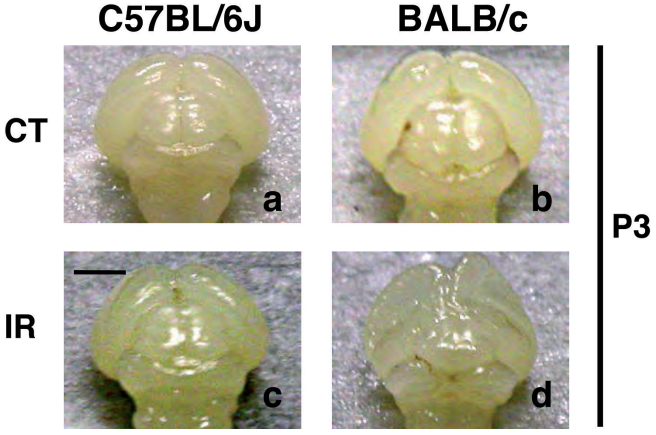

Fig. 1. Gross appearance of the cerebellum at P3. Control C57BL/6J (**a**), control BALB/c (**b**), irradiated C57BL/6J (**c**), and irradiated BALB/c (d). Midline part of the cerebellum in the irradiated BALB/c (**d**) is remarkably hypoplastic compared to controls (**a, b**) and the irradiated C57BL/6J (**c**). CT: Non-irradiated control, IR: Irradiated. Scale bar: 3 mm.

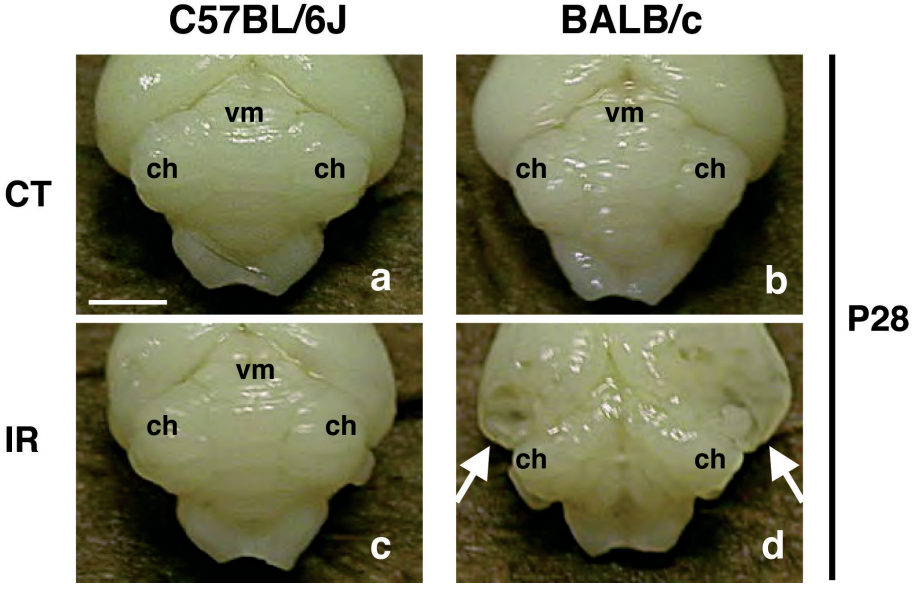

Fig. 2. Gross appearance of the cerebellum at P28. Control C57BL/6J (**a**), control BALB/c (**b**), irradiated C57BL/6J (**c**), and irradiated BALB/c (**d**). The irradiated BALB/c (**d**) shows almost complete defect of the cerebellar vermis, though no obvious abnormality is observed in the cerebellum of the irradiated C57BL/6J (**c**). Arrows indicate the hydrocephalus in the irradiated BALB/c (**d**). vm: vermis, ch: cerebellar hemisphere. Scale bar: 5 mm.

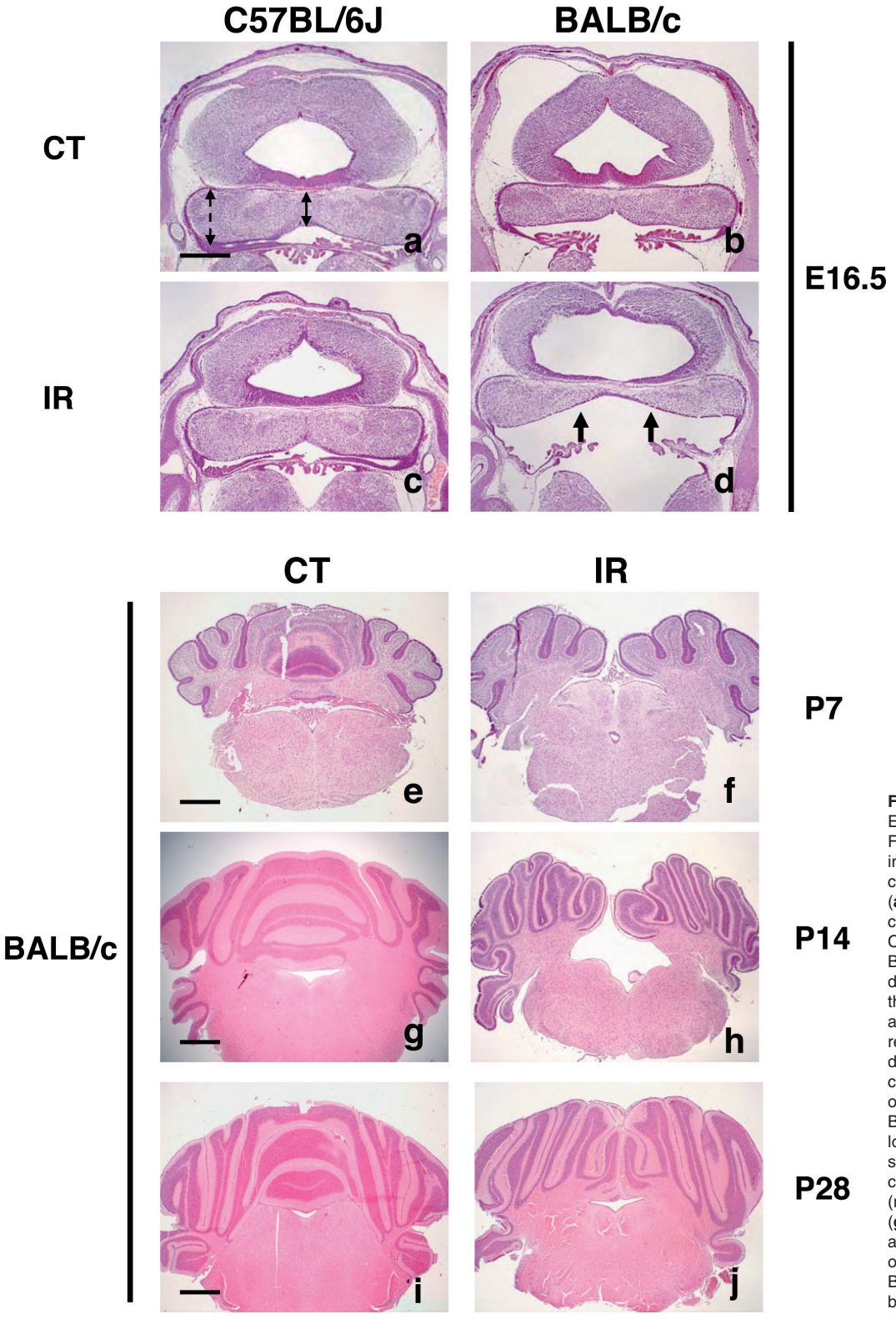

Fig. 3. Coronal section from E16.5, P7, P14 and P28. Figures in the upper panel indicate coronal sections of the cerebellum from E16.5 embryo (**a-d**). Control C57BL/6J (**a**), control BALB/c (**b**), irradiated C57BL/6J (**c**), and irradiated BALB/c (**d**). A solid arrow and a dotted arrow indicate the thickness of the midline part and the hemispheres, respectively (**a**). A notable decrease in the thickness of the cerebellum (arrows) was observed in the irradiated BALB/c (**d**). Figures in the lower panel indicate coronal sections of the cerebellum from control (left) and irradiated (right) BALB/c. P7 (**e, f**), P14 (**g, h**), and P28 (**i, j**). An apparent deficit of the vermis is observed in the irradiated BALB/c mice. HE stain. Scale bars: a-d, 20 μm; e-j, 500 μm.

were probably neural stem cells or neural progenitors just differentiated from stem cells. A few pyknotic cells were also observed in the VZ of irradiated C57BL/6J (Fig. 5c). The distribution of the pyknotic cells was diffuse in both strains. In control animals of both strains, almost no pycnotic cells were observed (Fig. 5a,b).

At E16.5, a notable increase in thickness of the midline part of the cerebellum was observed in the control animals of both strains (Fig. 3a,b) and irradiated C57BL/6J (Fig. 3c). On the other hand, the thickness of the midline part in irradiated BALB/c did not increase, despite normal development of the cerebellar hemispheres (Fig. 3d).

At E18.5, the midline part of the cerebellum in the control animals became even thicker, and the EGL and the Purkinje cell layer (PCL) appeared (Fig. 5e,f). These two layers were also observed in the irradiated C57BL/6J, though they were rather thin compared to the control (Fig. 5g). In contrast, the development of the midline part and generation of two cell layers were hardly seen in the irradiated BALB/c (Fig. 5h). At the cerebellar hemispheres, however, EGL and PCL were formed even in the irradiated BALB/c, though their thickness was slightly reduced compared to that of the control animals (data not shown).

At P0, though formation of the two layers proceeded in the control animals of both strains and irradiated C57BL/6J, there was no obvious formation of the cell layers in the midline cerebellum of the irradiated BALB/c (Fig. 5i-l).

Through embryogenesis from E14.5 to P0, development of the cerebellar hemispheres was not affected by irradiation in either strain (Fig. 6a). On the other hand, there was a reduction in the thickness of the midline part of the irradiated cerebellum compared to the control animals at each time point in both strains. The reduction was more prominent in the irradiated BALB/c. (Fig. 6b).

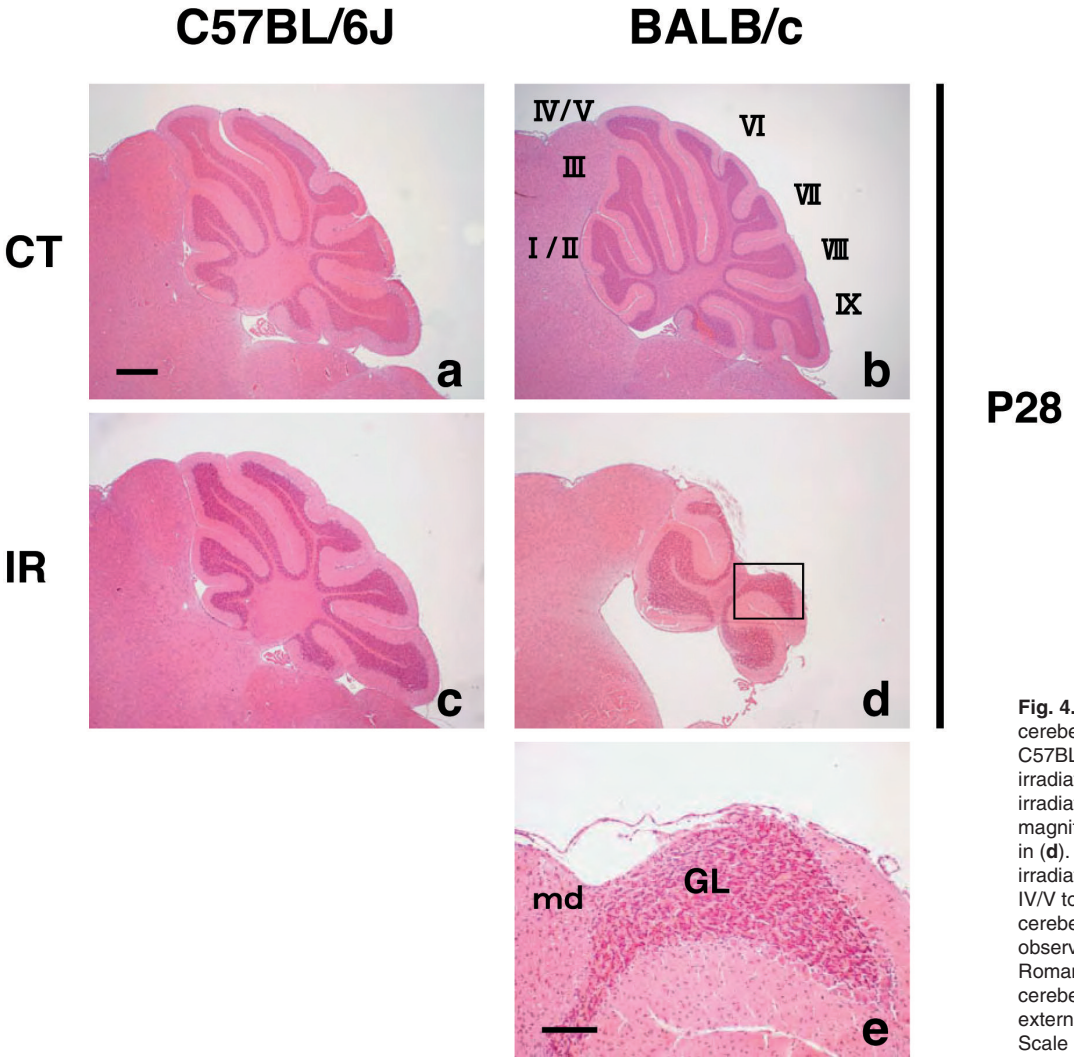

Fig. 4. Midline sections of the cerebellum from P28 mice. Control C57BL/6J (**a**), control BALB/c (**b**), irradiated C57BL/6J (**c**), and irradiated BALB/c (**d**). **e** is a higher magnification from the squared area in (**d**). Defected areas in the irradiated BALB/c extend from lobule IV/V to lobule VIII (**d**). Denudation of cerebellar medulla and EGL was observed in the defected area (**e**). Roman figures indicate each cerebellar lobule. md: medulla, EGL: external germinal layer. HE stain. Scale bars: a-d, 500μm; e, 100 μm.

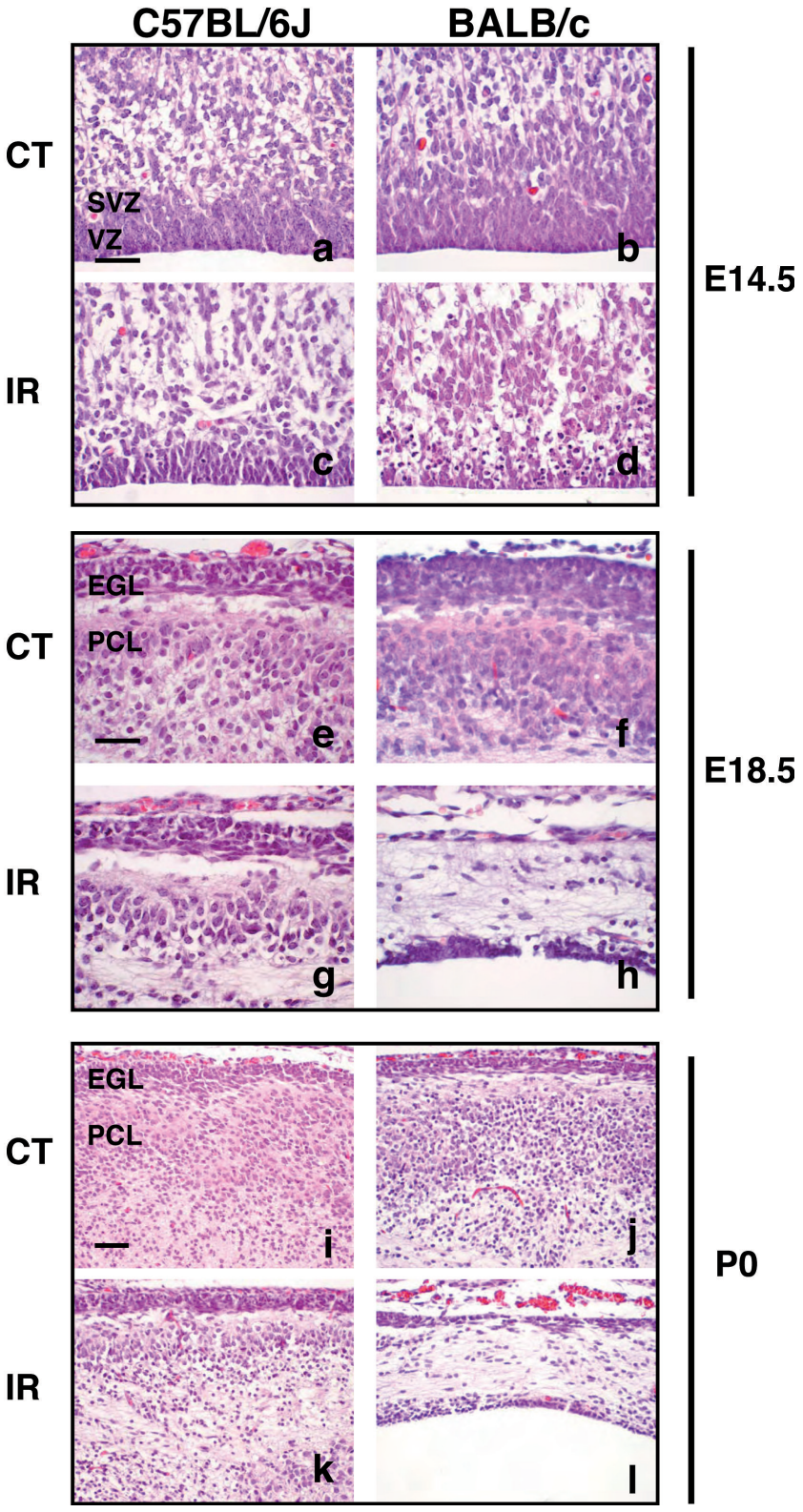

Fig. 5. Higher magnification of the midline part of the cerebellum. E14.5 (**a-d**), E18.5 (**e-h**), and P0 (**i-l**). Sections from C57BL/6J (left) and BALB/c (right). A number of pyknotic cells were observed in the VZ of BALB/c mice 24 hours after irradiation (E14.5) (**d**). EGL and PCL were hardly observed in the irradiated BALB/c at E18.5 and P0 (**h, l**). VZ: ventricular zone, SVZ: subventricular zone, EGL: external germinal layer, PCL: Purkinje cell layer. HE stain. Scale bars: a-h, 40 μm; i-l, 50 μm

At P7, the developing vermis was clearly observed in the control animals (Fig. 3e) and the irradiated C57BL/6J (data not shown), and a formation of the vermis was almost completed at P28 (Fig. 3g,i). On the other hand, in the irradiated BALB/c, though the development of the cerebellar hemispheres could be

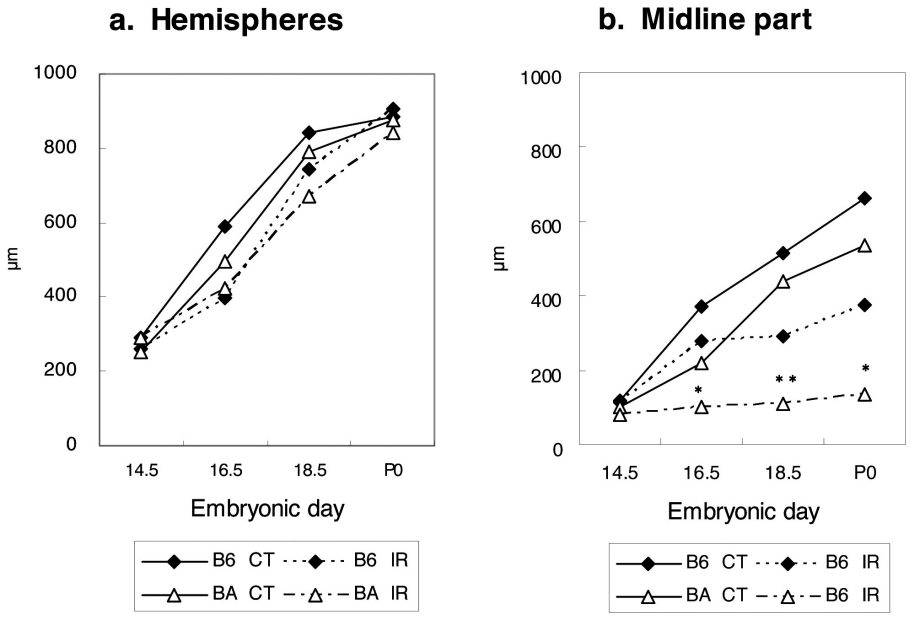

Fig. 6. Thickness of the hemispheres (**a**) and midline part (**b**) of the cerebellum. There was no difference in the thickness of the cerebellar hemispheres between control animals and irradiated animals in any strains. On the other hand, there was a reduction in the thickness of the midline part of the irradiated cerebellum compared to the control at each time point. The reduction was more prominent in the irradiated BALB/c. *: $p<0.05$ (Student's t-test). **: $p<0.01$ (Student's t-test) vs. control.

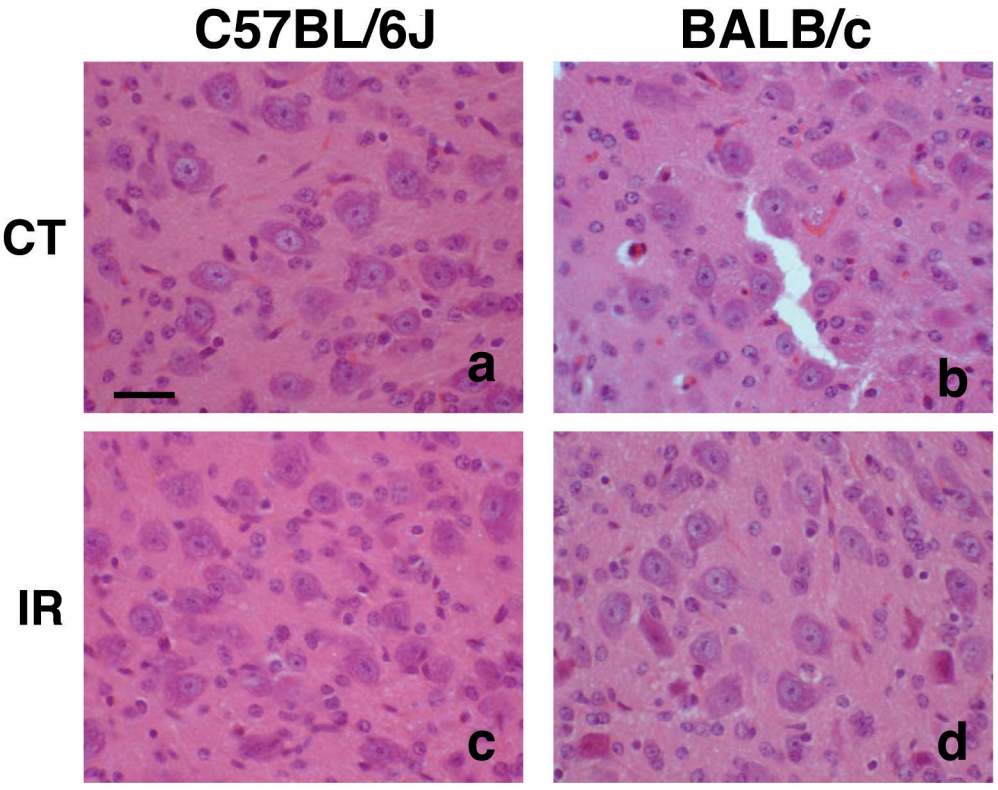

Fig. 7. Neurons in the cerebellar nuclei of the cerebellum from P21 mice. Control C57BL/6J (**a**), control BALB/c (**b**), irradiated C57BL/6J (**c**), and irradiated BALB/c (**d**). No obvious change was observed in the number of the neurons in the cerebellar nuclei after irradiation. Scale bar: 20 μm.

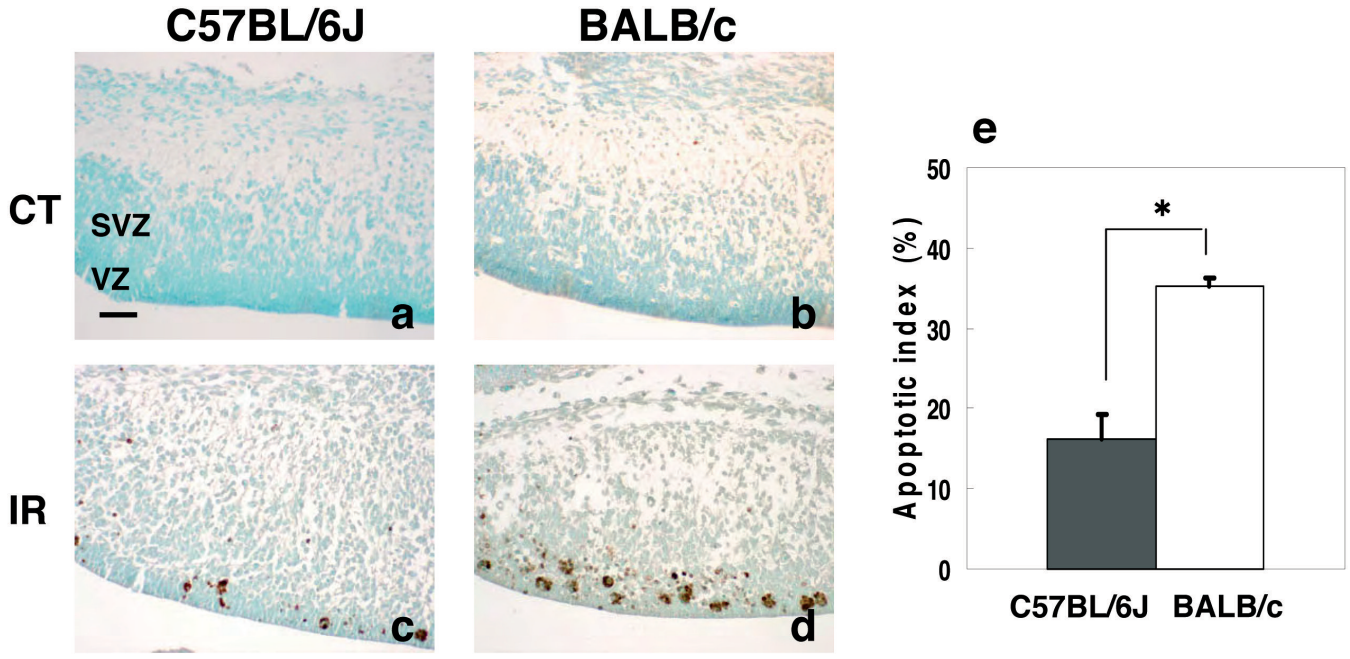

Fig. 8. TUNEL-stained sections of the cerebellum 24 hours after irradiation (**a-d**). Control C57BL/6J (**a**), control BALB/c (**b**), irradiated C57BL/6J (**c**), and irradiated BALB/c (**d**). A number of TUNEL-positive cells were observed in the VZ of irradiated BALB/c (**d**), while a few cells were TUNEL-positive in that of C57BL/6J. VZ: ventricular zone, SVZ: subventricular zone. Scale bar: 40 μm. Apoptotic index in both VZ and SVZ of irradiated BALB/c and C57BL/6J mice 24 hours after irradiation (**e**). The apoptotic index of Irradiated BALB/c is significantly higher than that of C57BL/6J *: $p<0.05$ (Student's t-test), irradiated BALB/c vs. irradiated C57BL/6J.

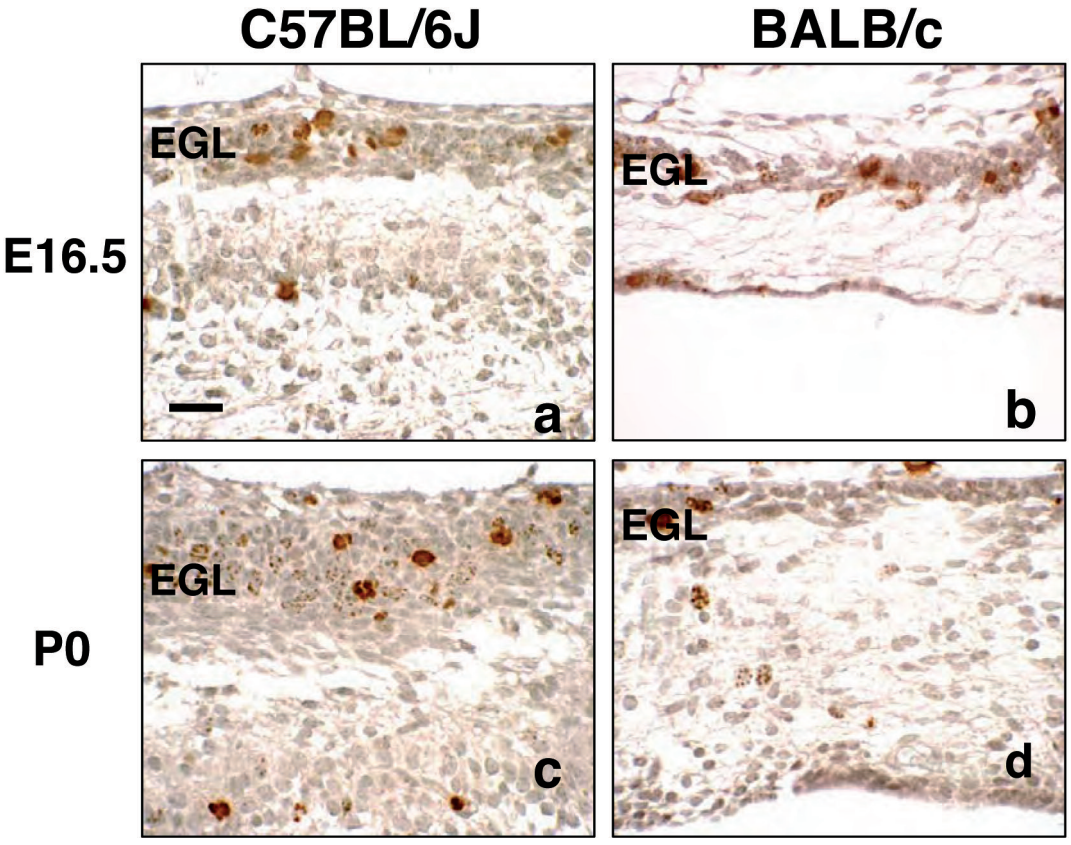

Fig. 9. pH3 immunostain of EGL from E16.5 (**a, b**) and P0 (**c, d**). Irradiated C57BL/6J (left) and irradiated BALB/c (right). Positive cells were distributed mainly at EGL. EGL: external germinal layer. Scale bar: 40 μm.

observed, there was no formation of the vermis at P7 and thereafter (Fig. 3f). The development of both cerebellar hemispheres normally progressed without formation of the vermis, and the developed cerebellar hemispheres contacted one another at the midline of the cerebellum (Fig. 3h,j). At P28, in the cerebellum of irradiated BALB/c, the size of the whole hemisphere was not different from the normal one, but there was an increase in the number of folia (Fig. 3i,j).

At a midline section of P28 in the irradiated BALB/c, the defect extended from lobule IV/V to lobule VIII (Fig. 4a-d). Around these areas, denudation of the granular layer was observed, because of a deficit of the molecular layer that covers the cerebellar surface in the controls. Moreover, in parts, even the granular layer defected and the cerebellar medulla denudated (Fig. 4e). In contrast to the severe patterning disorder of the cell layers, there was no obvious change in the number of neurons in the cerebellar nuclei (Fig. 7).

Induction of apoptosis

There were a number of pyknotic cells in the cerebellum of irradiated BALB/c 24 hours after irradiation (Fig. 5d). In order to verify the hypothesis that the vermis defect in the irradiated BALB/c is caused by excessive cell death in the periventricular wall induced by irradiation, we applied the TUNEL method for E14.5 sections. No or very few TUNEL-positive cells were observed in the control animals (Fig. 8a,b), while there were a number of positive cells around the VZ in the irradiated BALB/c (Fig. 8d), corresponding with the distribution of the pyknotic cells on HE sections. The TUNEL-positive cells were also observed in irradiated C57BL/6J, but the number was relatively low compared to the irradiated BALB/c (Fig. 8c). There was a significant strain difference in the percentage of the TUNEL-positive cells (Fig. 8e). On the other hand, there were a few positive cells in the rhombic lip, where the granule cell precursors arise, in the two strains (data not shown). In the EGL, where the granule cell precursors migrate from the rhombic lip and proliferate, no positive cells were detected (data not shown). These results suggest that BALB/c is sensitive to irradiation and tends to undergo apoptosis in a specific part of cerebellar anlage.

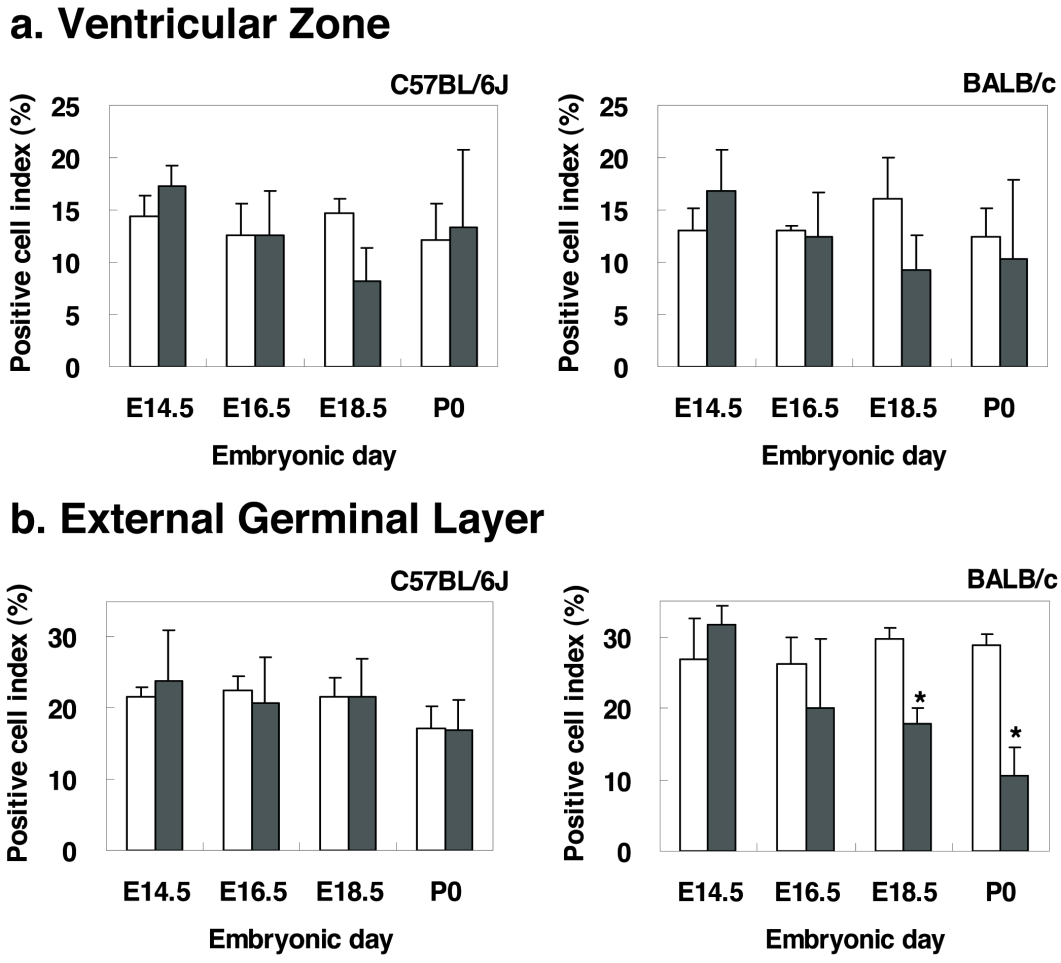

Fig. 10. pH3-positive cell index in the VZ (**a**) and EGL (**b**). Positive cell index in BALB/c tended to decrease after irradiation, showing a significant decrease especially in EGL at E18.5 and P0 (**b**). Non-irradiated control (white bars) and irradiated (black bars) animals. *: $p<0.05$ (Student's t-test) vs. control.

Proliferation activity

As we assumed that the irradiation affected cell proliferation during cerebellar development and resulted in the morphological abnormality, we then conducted immunostaining for pH3 from E14.5 to P0.

pH3-positive cells were distributed at the VZ and EGL in both strains (Fig. 9). No significant difference in the percentage of pH3 positive cells was observed in C57BL/6J between control and irradiated animals. In contrast, the positive cell index tended to decrease in irradiated BALB/c compared to the control at each time point, and significantly decreased at E18.5 and P0 in the EGL (Fig. 10).

Discussion

The present study demonstrated that the γ-irradiation of 1.5 Gy on BALB/c mice at E13.5 induced a severe deficit of the cerebellar vermis. The cerebrum in this period of embryogenesis is extremely susceptible to irradiation, and a number of studies have revealed that irradiation on E13.5 caused a variety of cerebral abnormalities dose-dependently, such as neuronal apoptosis, heterotopias, reduced brain weight, thinning of the cerebrum cortex, and hydrocephalus (Fukui et al., 1991). As for the cerebellum, however, a prenatally irradiated rat at this period of embryogenesis showed migration abnormalities of the Purkinje cells and granule cells, or foliation abnormalities (Inouye and Kameyama, 1983, 1986; Inouye et al., 1992), but no macroscopic abnormalities in the cerebellum after birth. Cerebellar abnormality induced by irradiation at E13.5 in the present study is conceivable by thinking of the murine developmental stage, because this period corresponds to the stage of formation of the two cell layers, Purkinje cell and granule cell layers (Hatten, 1999; Sotelo, 2004).

There was a greater increase of TUNEL-positive cells in the cerebellum of irradiated BALB/c 24 hours after the irradiation compared to C57BL/6J (Fig. 8). Also, proliferation activity was suppressed in irradiated BALB/c (Fig. 10). It is well known that neuronal stem cells and progenitor cells show a high incidence of apoptosis caused by irradiation through neurogenesis, because of its radiosensitivity. It is also considered that insults to such cell groups lead to a disturbance of cell proliferation/migration during neurogenesis, resulting in histological aberration observed after birth. In fact, Inouye et al. reported heterotopias of granule cells, and Darmanto et al. of Purkinje cells. In their studies, irradiation was conducted at P3 in ICR mice and E21 in Wister rats, respectively, when differentiation of these precursor cells has already completed and starts its migration (Inouye et al., 1992; Darmanto et al., 2000). Moreover, it has also been pointed out that postnatal histological anomaly of the central nervous system in irradiated fetuses is caused by apoptotic changes around the VZ soon after irradiation (Sun et al., 1996; Aolad et al., 2000; Darmanto et al., 2000; Kubota et al., 2000). In these reports, morphological changes of the cerebrum such as microcephalus and hydrocephalus were observed after irradiation at E7 to E13 in ICR mice. As compared to these reports, irradiation time point in the present study was E13.5, which just corresponds to the developmental stage of the cerebellum where the progenitor cells proceed after their differentiation and migration (Altman, 1972; Altman and Bayer, 1978, 1985; Hatten, 1999; Sotelo, 2004). Apoptotic cell distribution around the VZ also supports the aforementioned process of vermis deficit (Figs. 5a-d, 8 a-d). That is, the result of this experiment leads to the speculation that highly evoked apoptosis of the neural stem and/or progenitor cells around VZ in BALB/c fetuses by irradiation caused the disturbance of cell proliferation/migration, and following cerebellar vermis deficit.

From histological analysis at E18.5 and P0, severe losses of Purkinje cells and granule cells were observed, and there may be an involvement of the interaction between Purkinje cells and granule cells during cerebellar development. Purkinje cell progenitors arise from the VZ at E11-13, and migrate to the surface of the cerebellum at E12-15 to form PCL (Hatten 1999; Sotelo, 2004). Thus, we can assume that the absence of Purkinje cells in BALB/c vermis anlage is due to the irradiation insult to the Purkinje cell progenitors and following apoptosis in the VZ at E13.5. During normal cerebellar development, Purkinje cells enhance the proliferation of granule cells in EGL after formation of its own cell layer (Wetts and Herrup, 1982; Sonmez et al., 1984; Herrup and Sunter, 1987). Stimulated by Purkinje cells, granule cells proliferate explosively, and due to this proliferation of granule cells the cerebellum undergoes over a 1000-fold increase in volume, and formation of characteristic fissures and folia occurs simultaneously. This mitogenic effect of Purkinje cells on granule cells is mediated by sonic hedgehog (Shh), a secreted factor expressed in Purkinje cells. There are a series of experiments demonstrating that the inhibition of Shh in the developing cerebellum caused reduction in the number of granule cells in EGL, and subsequent loss of foliations or cerebellar malformation (Dahmane and Ruiz i Albata, 1999; Wallace, 1999; Wechsler-Reya and Scott, 1999; Lewis et al., 2004; Corrales et al., 2006). Therefore, irradiation insult on Purkinje cell progenitors in VZ caused the reduction of Shh secretion. In response to Shh deficiency, granule cell proliferation was suppressed and abnormal foliation and macroscopic aberration of cerebellum occurred. To prove this, we have to examine the secretion of Shh after irradiation.

Besides Shh, the genetic mechanisms that are involved in the cerebellar development were recently revealed (Herrup and Kuemerle, 1997). Among them, the zinc-finger transcription factor Zfp423 is considered to play a crucial role in the patterning of neuronal and glial precursors of the developing cerebellum, especially in the midline structure (Alcaraz et al., 2006). Alcaraz et al. using Zfp423-deficient mice which display severe

vermis malformation, showed that Zfp423 is required for proliferation and differentiation of neuron and radial glia, with selective vulnerability at the midline. This raises the possibility that the irradiation may affect the genetic mechanism of the cerebellar development, and finally result in the focal defect of the vermis.

Though apoptotic cells were dispersed throughout the VZ 24 hours after irradiation, morphological abnormalities in the irradiated BALB/c were restricted only to the vermis on postnatal days, and the other parts of the cerebellum were almost normal (Fig. 2d). The question arises of why the postnatal abnormality is restricted only to the vermis. One possible cause is a contribution of Mediolateral (M-L) clusters during the cerebellar development. Many of the early anatomical and physiological studies revealed that the cerebellar cortex is compartmentalized into a series of bilaterally symmetric clusters along the mediolateral axis (Voogd and Ruigrok, 1997, Voogd and Glickstein, 1998; Garwicz, 2000). M-L clusters play important roles not only as basic units of cerebellar function, but also as units of the morphological development and formation of the neural network (Hawkes and Gravel, 1991, 1993; Leclerc et al., 1992; Hawkes, 1997; Herrup and Kuemerle, 1997; Oberdick et al., 1998). Hashimoto (2003), reported that a cluster comprising the midline part of the cerebellum, where vermis defect was observed in the present experiment, is formed by Purkinje cell progenitors differentiated at E12.5. Therefore, it is possible that the irradiation injured only more sensitive Purkinje cell progenitors just after the differentiation, causing a focal loss of granule cells and further morphological deficit of the cerebellar vermis. A more complete study needs to be performed to confirm this speculation, but from this viewpoint, irradiation at another time point may induce abnormalities in another area of the cerebellum. For example, as Purkinje cells of the cerebellar hemispheres generate earlier than those of the vermis (i.e., E11-12) (Altman and Bayer, 1985; Hashimoto and Mikoshiba, 2003), irradiation at this period may elicit abnormalities of the cerebellar hemisphere.

In contrast to the severe patterning disorder of the cell layers, there was no obvious change in the number of neurons in the cerebellar nuclei. Neurons in the cerebellar nuclei arise from the VZ as well as the Purkinje cells, but slightly before the generation of the Purkinje cell precursors (Altman and Bayer, 1978; Sotelo, 2004). The irradiation time point in the present study was at E13.5, when the generation of neurons in the cerebellar nuclei is over, but the Purkinje cell precursors still continue to differentiate. Therefore, this result also supports the above-mentioned hypothesis that the irradiation injured only more sensitive Purkinje cell precursors just after the differentiation.

Differences in radiosensitivity among various mouse strains are well recognized, and among them, BALB/c is found to be unusually sensitive to the lethal effect of the irradiation, particularly compared to C57BL/6 mice (Grahn and Hamilton, 1957). Recently, it was shown that the radiosensitivity of BALB/c mice was caused by the accumulation of DNA double strand break (DSB) in the genome as a result of non-homologous end joining (NHEJ) failure (Okayasu et al., 2000). BALB/c mice have a mutation in the *DNA-PKcs* gene, which is an important factor in NHEJ mechanism, and it may cause DSB repair deficiency (Yu et al., 2001).

The present study demonstrated that prenatal irradiation can be a crucial cause of cerebellar vermis deficit in BALB/c mice. Though it has been common knowledge that the cerebellar anlage in early embryogenesis is not susceptible to irradiation, the present results clearly indicate that progenitor cells in the anlage can be susceptible, depending on the potential factor, such as radiosensitivity in BALB/c strain. To elucidate such factors may contribute to progress in the field of developmental toxicology.

Acknowledgements. We wish to thank Mayumi Shinagawa, Eriko Shishikura, Yumiko Sugawara and Mutsumi Kaminishi for animal care.

References

Alcaraz W.A., Gold D.A., Raponi E., Gent P.M., Concepcion D. and Hamilton B.A. (2006). Zfp423 controls proliferation and differentiation of neural precursors in cerebellar vermis formation. Proc. Natl. Acad. Sci. USA 103, 19424-19429.

Altman J. (1972). Postnatal development of the cerebellar cortex in the rat. I. The external germinal layer and the transitional molecular layer. J. Comp. Neurol. 145, 353-397.

Altman J. and Bayer S.A. (1978). Prenatal development of the cerebellar system in the rat. I. Cytogenesis and histogenesis of the deep nuclei and the cortex of the cerebellum. J. Comp. Neurol. 179, 23-48.

Altman J. and Bayer S.A. (1985). Embryonic development of the rat cerebellum. III. Regional differences in the time of origin, migration, and settling of Purkinje cells. J. Comp. Neurol. 231, 42-65.

Aolad H.M., Inouye M., Darmanto W., Hayasaka S. and Murata Y. (2000). Hydrocephalus in mice following X-irradiation at early gestational stage: possibly due to persistent deceleration of cell proliferation. J. Radiat. Res. (Tokyo) 41, 213-226.

Corrales J.D., Blaess S., Mahoney E.M. and Joyner A.L. (2006). The level of sonic hedgehog signaling regulates the complexity of cerebellar foliation. Development 133, 1811-1821.

Dahmane N. and Ruiz i Altaba A. (1999). Sonic hedgehog regulates the growth and patterning of the cerebellum. Development 126, 3089-3100.

Darmanto W., Inouye M., Takagishi Y., Ogawa M., Mikoshiba K. and Murata Y. (2000). Derangement of Purkinje cells in the rat cerebellum following prenatal exposure to X-irradiation: decreased Reelin level is a possible cause. J. Neuropathol. Exp. Neurol. 59, 251-262.

Fukui Y., Hoshino K., Hayasaka I., Inouye M. and Kameyama Y. (1991). Developmental disturbance of rat cerebral cortex following prenatal low-dose gamma-irradiation: a quantitative study. Exp. Neurol. 112, 292-298.

Garwicz M. (2000). Micro-organisation of cerebellar modules controlling

forelimb movements. Prog Brain Res. 124, 187-199.

Grahn D. and Hamilton K.F. (1957). Genetic variation in the acute lethal response of four inbred mouse strains to whole body X-irradiation. Genetics 42, 189-198.

Hashimoto M. and Mikoshiba K. (2003). Mediolateral compartmentalization of the cerebellum is determined on the "birth date" of Purkinje cells. J. Neurosci. 23, 11342-11351.

Hatten M.E. (1999). Central nervous system neuronal migration. Annu. Rev. Neurosci. 22, 511-539.

Hawkes R. (1997). An anatomical model of cerebellar modules. Prog. Brain Res. 114, 39-52.

Hawkes R., Blyth S., Chockkan V., Tano D., Ji Z. and Mascher C. (1993). Structural and molecular compartmentation in the cerebellum. Can. J. Neurol. Sci. 20 (Suppl 3), S29-35.

Hawkes R. and Gravel C. (1991). The modular cerebellum. Prog. Neurobiol. 36, 309-327.

Herrup K. and Kuemerle B. (1997). The compartmentalization of the cerebellum. Annu. Rev. Neurosci. 20, 61-90.

Herrup K. and Sunter K. (1987). Numerical matching during cerebellar development: quantitative analysis of granule cell death in staggerer mouse chimeras. J. Neurosci. 7, 829-836.

Hoshino K. and Kameyama Y. (1988). Developmental-stage-dependent radiosensitivity of neural cells in the ventricular zone of telencephalon in mouse and rat fetuses. Teratology 37, 257-262.

Inouye M. and Kameyama Y. (1983). Cell death in the developing rat cerebellum following X-irradiation of 3 to 100 rad: a quantitative study. J. Radiat. Res. (Tokyo) 24, 259-269.

Inouye M. and Kameyama Y. (1986). Long-term neuropathological consequences of low-dose X-irradiation on the developing rat cerebellum. J. Radiat. Res. (Tokyo) 27, 240-246.

Inouye M., Hayasaka S., Funahashi A. and Yamamura H. (1992). Gamma-radiation produces abnormal Bergmann fibers and ectopic granule cells in mouse cerebellar cortex. J. Radiat. Res. (Tokyo) 33, 275-281.

Kameyama Y. (1982). Low-dose radiation as an environmental agent affecting intrauterine development. Environ. Med. 26, 1-15.

Kameyama Y., Hayashi Y. and Hoshino K. (1972). Long-term pathological effects of prenatal x-radiation on the developing brain--abnormal vascularity in the brain mantle of x-ray induced microcephaly of the mouse. Annu. Rep. Res. Inst. Environ. Med. Nagoya Univ. 19, 75-83.

Kameyama Y. and Hoshino K. (1986). Sensitive phase of CNS development. New York, Stuttgart.

Kubota Y., Takahashi S., Sun X.Z., Sato H., Aizawa S. and Yoshida K. (2000). Radiation-induced tissue abnormalities in fetal brain are related to apoptosis immediately after irradiation. Int. J. Radiat. Biol. 76, 649-659.

Leclerc N., Schwarting G.A., Herrup K., Hawkes R. and Yamamoto M. (1992). Compartmentation in mammalian cerebellum: Zebrin II and P-path antibodies define three classes of sagittally organized bands of Purkinje cells. Proc. Natl. Acad. Sci. USA 89, 5006-5010.

Lewis P.M., Gritli-Linde A., Smeyne R., Kottmann A. and McMahon A.P. (2004). Sonic hedgehog signaling is required for expansion of granule neuron precursors and patterning of the mouse cerebellum. Dev. Biol. 270, 393-410.

Miale I.L. and Sidman R.L. (1961). An autoradiogrphic analysis of histogenesis in the mouse cerebellum. Exp. Neurol. 4, 277-296.

Oberdick J., Baader S.L. and Schilling K. (1998). From zebra stripes to postal zones: deciphering patterns of gene expression in the cerebellum. Trends Neurosci. 21, 383-390.

Okayasu R., Suetomi K., Yu Y., Silver A., Bedford J.S., Cox R. and Ullrich R.L. (2000). A deficiency in DNA repair and DNA-PKcs expression in the radiosensitive BALB/c mouse. Cancer Res. 60, 4342-4345.

Sonmez E. and Herrup K. (1984). Role of staggerer gene in determining cell number in cerebellar cortex. II. Granule cell death and persistence of the external granule cell layer in young mouse chimeras. Brain Res. 314, 271-283.

Sotelo C. (2004). Cellular and genetic regulation of the development of the cerebellar system. Prog. Neurobiol. 72, 295-339.

Sun X., Inouye M., Takagishi Y., Hayasaka S. and Yamamura H. (1996). Follow-up study on histogenesis of microcephaly associated with ectopic gray matter induced by prenatal gamma-irradiation in the mouse. J. Neuropathol. Exp. Neurol. 55, 357-365.

Sun X.Z., Inouye M., Hayasaka I., Takagishi Y. and Yamamura H. (1995). Morphological alternations in radial glia cells following brain injury in fetal brain. Environ. Med. 39, 121-124.

Voogd J. and Glickstein M. (1998). The anatomy of the cerebellum. Trends Neurosci. 21, 370-375.

Voogd J. and Ruigrok T.J. (1997). Transverse and longitudinal patterns in the mammalian cerebellum. Prog. Brain. Res. 114, 21-37.

Wallace V.A. (1999). Purkinje-cell-derived Sonic hedgehog regulates granule neuron precursor cell proliferation in the developing mouse cerebellum. Curr. Biol. 9, 445-448.

Wechsler-Reya R.J. and Scott M.P. (1999). Control of neuronal precursor proliferation in the cerebellum by Sonic Hedgehog. Neuron 22, 103-114.

Wetts R. and Herrup K. (1982). Interaction of granule, Purkinje and inferior olivary neurons in lurcher chimaeric mice. I. Qualitative studies. J. Embryol. Exp. Morphol. 68, 87-98.

Yu Y., Okayasu R., Weil M.M., Silver A., McCarthy M., Zabriskie R., Long S., Cox R. and Ullrich R.L. (2001). Elevated breast cancer risk in irradiated BALB/c mice associates with unique functional polymorphism of the Prkdc (DNA-dependent protein kinase catalytic subunit) gene. Cancer Res. 61, 1820-1824.

Accepted February 13, 2008